

## Extreme Rainfalls in the Southern Alps of New Zealand

R D Henderson <sup>1</sup> and S M Thompson <sup>2</sup>

*National Institute of Water and Atmospheric Research Ltd.,*

<sup>1</sup> *P O Box 8602, Christchurch and*

<sup>2</sup> *P O Box 14901, Wellington, New Zealand*

### Abstract

We report on the most intense rainfalls observed in the Southern Alps over durations of 6 minutes to one year, and find two notable features attributable to the orographic nature and maritime location of the rainfall. Firstly the onset and end of intense rain events are nearly simultaneous over the 400 km length of the mountain barrier. Secondly the quantities "maximum intensity times the square root of the duration", for durations of approximately one day and one year, are substantially greater than those for the other durations in this range.

An examination of the spatial distribution of storm rain depths and normal rain indicates that the maxima are all from a zone up to 10 km wide and extending (perhaps intermittently) for 400 km along the north west side of the mountains. The location of this narrow strip is the same relative to the Alpine Fault on four trans-alpine profiles 100 km apart, and the magnitude of the maximum rain is related to the elevation of the Main Divide in the vicinity of each profile.

### Introduction

In many parts of the world, the contribution of mountain areas to water resources is large in proportion to their areal extent, due to orographic enhancement of precipitation. This greater contribution occurs across the discharge spectrum, from high flows, where orographic enhancement frequently contributes to floods, to low flows, where water stored as snow and ice is released in spring and summer. In New Zealand, the headwaters of most major rivers are mountainous. The average rainfall distribution reflects both the presence of mountains, and the prevailing direction of moisture bearing-winds, with enhancement on the upwind side and a rain shadow on the downwind side (Grant, 1969; McSaveney, 1978; McSaveney et al., 1978; Chinn, 1979; New Zealand Meteorological Service, 1983; Griffiths and

McSaveney, 1983). The dominance of mountainous parts of catchments is also reflected in studies of water balance (Coulter, 1973) and storm rain intensity (Tomlinson, 1980; Whitehouse, 1985; Henderson, 1993).

A stimulus for research on Southern Alps rainfall has come from the need to better estimate probable maximum precipitation (PMP). These maxima are of concern to regional governments, which have responsibilities for flood protection and dam safety, and to dam owners. Maximum precipitation levels in the Southern Alps can influence the national economy, as nearly 50% of electricity generation and 76% of the hydroelectric storage relies on dams on rivers draining the Southern Alps (Electricity Shortage Review Committee, 1992).

Near the Main Divide of the Southern Alps the mean precipitation is very large (up to c. 14 m/y) and storms are frequent, although seasonal and inter-annual variations are minor, reflecting the maritime climate (Hessell 1982). However precipitation was not effectively measured until late in the 1970's (Chinn 1979), and this lack of data was evident in hydrological reports on rivers draining from the Main Divide. Stephen (1972) in a study of the Rakaia River, and Jowett and Thompson (1977), of the Clutha River, both found that the published maps underestimated the precipitation. Their conclusions were based on measured river flows southeast of the Main Divide. Duncan (1992) found the same for the Hokitika River, which flows northwest from the Main Divide. The problem is thus not only about the amount of precipitation down wind of the Main Divide, but a more general issue of estimation of precipitation on mountainous catchments.

Snow surveys were begun in the 1960's to better predict seasonal discharge to hydro storage reservoirs. The surveys proved difficult because of the rugged terrain and because unexpectedly high rainfalls interspersed with the snow falls made it impossible to effectively measure the snow component of the precipitation (Anderton, 1973; National Water and Soil Conservation Organisation, 1970-1975).

Rain measurements of up to 12 m/y, first measured in the 1970's, were used by Adams (1980) to explain a rate of erosion large enough to balance ~10 mm/y tectonic uplift inferred from other data by Wellman (1979).

Rain gauges in the Southern Alps are few in number (Fig. 1) and unevenly distributed, and the gauges may undercatch rainfall by up to 30% and snowfall by up to 80% (Rodda 1995). The amount of rain falling on the river catchments in the Southern Alps may thus be better determined by measuring river flow and adding an evaporation estimate to the measured runoff, as the evaporation (c. 0.7 m/y) is small compared to runoff (1.3 to 12.5 m/y) from catchments draining the Main Divide. It is not rain, but runoff, that is relevant to hydro-electricity, flood mitigation, and use of rivers for irrigation supply, waste disposal, wild habitat and recreation.

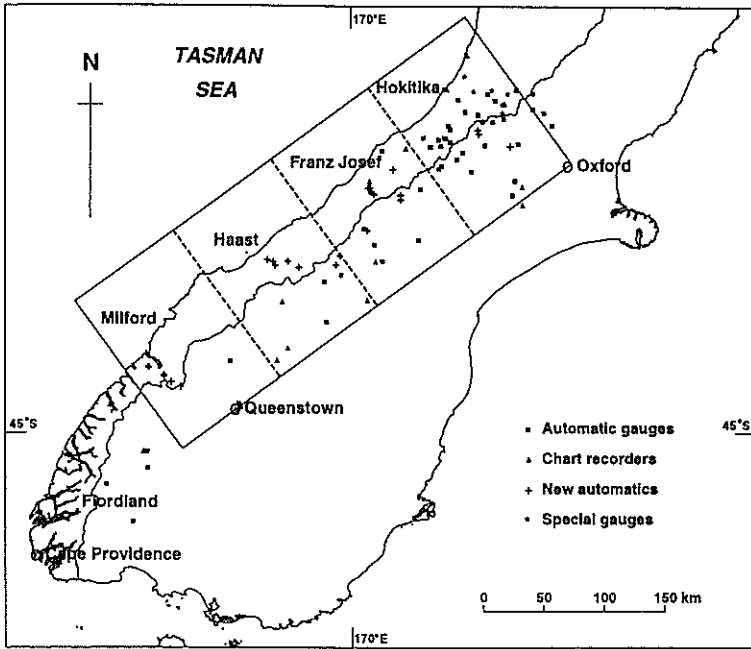


**FIGURE 1** – Map of the South Island, New Zealand showing locations of recording raingauges and trans-alpine profiles. The gauge types are: automatic tipping bucket with time resolution 6 or 15 minutes; charts with duration one day or one month; new automatics; and special gauges (disdrometer and drop counter) installed for short periods. The grid is based on the orientation of the Alpine Fault, which is approximately 85 km NW of the grid origin (marked as Cape Providence). The box is from 150 to 550 km NE and 0 to 150 km NW of grid origin. The new sites refer to gauges installed during this study.

However, rain gauge observations are still needed to determine the spatial variation of rain within the catchments, to understand the atmospheric processes that cause precipitation and to estimate the amount of precipitation stored as snow. Thus this paper focuses on the spatial distribution of rain, particularly during the most intense storms.

We test the hypothesis that precipitation is so influenced by orography that its spatial distribution is invariant and the heavier rain events occur simultaneously throughout the mountains.

## Study Region

The study region is a section of the Southern Alps extending 400 km NE from Fiordland (Fig. 1). The NW edge of this region is strikingly linear, as the mountains have been uplifted along the northeast-trending Alpine Fault, a major plate boundary. The ground rises steeply from the fault to the Main Divide.

The mountains form a barrier to the prevailing mid-latitude westerly winds, and the heaviest rain is associated with relatively warm air from the NW quarter. Figure 2 shows the height of the barrier formed by the mountain range: the traces represent the lowest and highest point every 10 km along the Main Divide, including higher points that are off the Main Divide. The average height of the barrier varies and is greatest in the Mount Cook region. The steepness of the terrain on the upwind side of the range is illustrated by four transects of ground elevation through the Alps at Franz Josef, near the highest point, Mt Cook (Fig. 3). The abruptness and the height of this mountain barrier influence the flow of moist air and the production of rain.

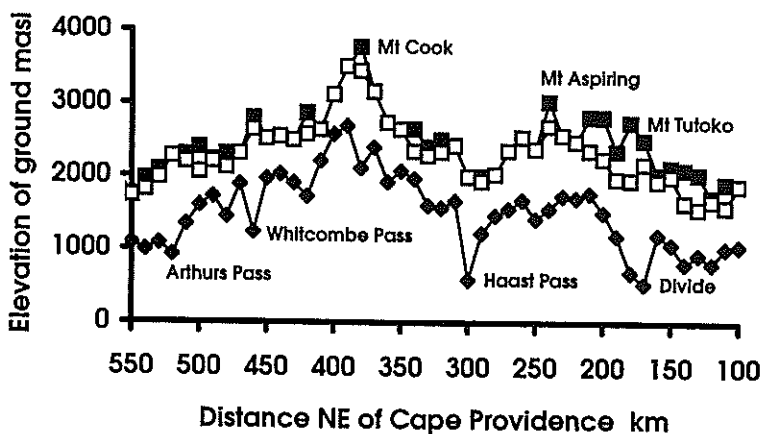


**FIGURE 2** – View of Southern Alps profile from the Tasman Sea, showing the section between 100 and 550 km NE along the study baseline (see Fig. 1). Line of filled diamonds is the lowest point along the Main Divide each 10 km. Open squares are the highest point in each 10 km. Filled squares are higher points off the divide. The low Whitcombe and Haast passes are oriented in a north-south direction, and are sheltered by high mountains from the prevailing northwest winds and the moisture they bring.

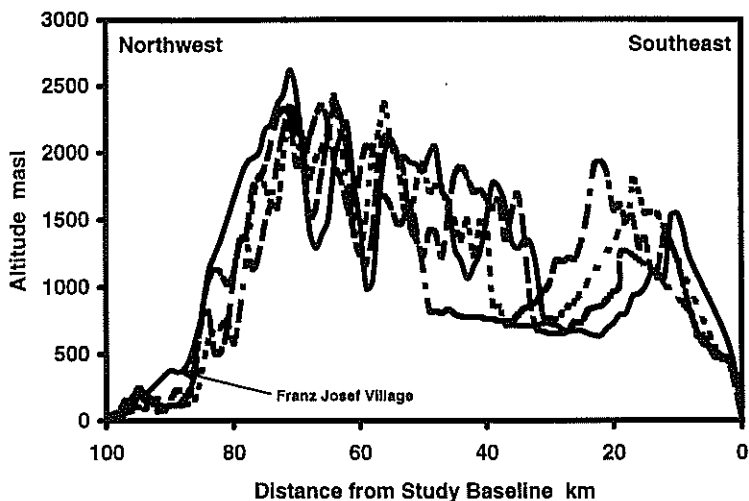


**FIGURE 3** – Transects of ground elevation in the vicinity of Franz Josef (see Fig. 1). The 4 lines represent transects 4 km apart and perpendicular to the Alpine Fault. Horizontal scale is km, with the Alpine Fault at 85 km, and the vertical scale is metres above sea level.

Northeast of the study area the Main Divide is lower, and uplift on the western side of the Alpine Fault has created additional ranges, such as the Paparoa Range, between the Tasman Sea and the Main Divide, creating complex rain shadows. Southwest of the study area, the Main Divide becomes lower, the coastline curves across the Alpine Fault, and the influence of other weather patterns becomes more pronounced.

To exploit the simple geometry of the study area, the rain data presented in this paper are plotted on a co-ordinate grid that has its major axis parallel to the Alpine Fault and 85 km SE of it (Fig. 1). The study area is 400 km long and 120 km wide, and for convenience of analysis has been divided into 4 equal parts; we plot the data from each part versus the NW co-ordinate as trans-alpine profiles. This area includes the catchments of the southern lakes and other rivers that drain SE from the Main Divide. The line of zero NW distance runs from Cape Providence in Fiordland through Queenstown to near Oxford. This line was chosen as the edge of a region beyond which significant NW rain rarely occurs.

## Data

In the mountains there is a network of automatic rain gauges located away from habitation and roads; their data are recovered by helicopter or radio

telemetry. Instruments are generally Ota tipping bucket gauges; early recorders used punched tape, but all recorders are now electronic. Storage gauges, including 3 m high PVC tubes, have been used in the alpine areas. In inhabited locations fringing the mountains, there are daily rain gauges and a few automatic gauges, such as Dines daily chart tilting-siphon gauges. Complete records are available for computer processing, except for some charts from which only the maximum rainfalls each month for a standard set of durations have been entered into a computer file.

A database of gauge locations (Walter 1990, with daily gauges added) was searched: 440 gauges were found within the study area, and we used the 261 that have more than one year of record. These are 45 automatic gauges with 351 station years; 147 daily gauges with 3107 station years; and 69 storage gauges with 972 station years of record. The locations of the 45 automatic gauges in the study area are shown in Figure 1.

A preliminary analysis prompted installation in 1991 of 12 new automatic gauges NW of the divide to confirm an hypothesis that the peak of the spatial distribution is between 5 and 15 km SE of the Alpine Fault. A new system for forecasting hydroelectric inflows was installed in 1994 and included 7 new automatic gauges sited ~3 km SE of the Main Divide to better monitor the high rainfall zone there.

## Methods

### Rain extremes

We seek information that will be of future use for estimating probable maximum precipitation (PMP), so we focused on the most extreme events, rather than on the annual series of extremes commonly used for frequency analysis and design storm derivation. The twelve largest non-overlapping rainfall totals for a range of durations from 6 minutes to 1 year were extracted from the data from each gauge (using the Tideda software package, Rodgers and Thompson, 1992, which takes account of all the time resolution available in the automatic records). A wide range of durations was analysed so that the results could be used for varied research problems (e.g. precipitation processes, snow storage, estimation of probable maximum floods and climate change).

More than 34000 rain totals of varying duration were produced. Not surprisingly, many were from the same large storms. Other rainfall totals were from gauges on the edges of the study area, and were contributed by storms that extended into the study area but did not affect the mountain catchments. To select a set of the most extreme rain storms, a measure of intensity that was independent of duration was required in order to rank the rain values and the storms they came from.

Extreme rainfalls from individual gauges, or from extensive regions are often presented by plotting rainfall versus duration on log-log axes. Enveloping lines are commonly drawn, of the form:

$$P_{\max} = X_n D^{-n} \quad (1)$$

where:

$P_{\max}$  = rainfall intensity for a specified duration in mm/h,

$D$  = duration in hours,

$n$  is an exponent describing the slope of a straight line on a log-log graph, and

$X_n$  is the intercept of this line at duration 1 hour, in mm/h.

Values of  $X_n$  and  $n$  vary according to geographic location and weather patterns. Table 1 shows a variety of  $X_n$  and  $n$  values proposed by a number of authors. Note that when  $P_{\max}$  is expressed as a rain depth in mm, the equivalent formula has exponent  $1-n$ .

In this analysis we use the parameter  $X_n$  as the measure of intensity to rank rain intensity maxima of differing durations. We choose  $n=0.5$  as a convenient value in the middle of the range proposed in the literature cited in Table 1. The list of 34000 rain intensity maxima was sorted into order of descending values  $X_{0.5}$ . Even though many maxima were from the same storms, there were too many to consider all events. A minimum value of  $X_{0.5} = 100$  was chosen to give a smaller number of extreme storms.

**TABLE 1** – Values of  $X$  and  $n$  from equation 1.

Reference	Region	$X$	$n$
Paulhus (1965)	World	421.6	0.525
Raudkivi(1979)	World	388.6	0.514
Shaw (1983)	World	425	0.53
Shaw (1983)	United Kingdom	96	0.57
Tomlinson (1980)	For New Zealand except Alps	112	0.447
Tomlinson (1980)	Southern Alps	190	0.447

## Data checking

Extreme rainfall values are sometimes due to data errors, and so a checking procedure was developed, using nearby gauges and the temporal information in the data. Extremes between six minutes and one hour duration were not verified against other gauges because for these time resolutions, we found that there was little relation among rainfalls at widely spaced gauges. Extremes of durations longer than 14 days were assumed to be correct as long as the period did not include any extremes of shorter duration that could not be checked.

There were 170 maxima from 36 individual storms with durations between two hours and 14 days, and values of  $X_{0.5} \geq 100$ . All 170 values were checked by plotting the available data from all gauges around the time of the extreme value. The rain intensity values were plotted at a time interval of one minute, in order to expose unusually large short-duration values, the most common error. Such errors occur when the punch tape mechanism of a tipping bucket recorder jams, when tapes are translated poorly, when manual data from check gauges are entered into the database without appropriate checking, or when a chart with an excessively steep gradient is digitised. Where data from a particular gauge appeared to be in error, the plots were reproduced on paper. Thirty-one extreme  $X_{0.5}$  values from eleven storms were rejected as data errors. The remaining 139 values (from 25 storms) with  $X_{0.5} \geq 100$  were all of duration 6 hours or longer.

Cumulative plots were used to check the temporal information in the rain data. The data from each automatic gauge were accumulated and divided by 0.001 times the individual gauge total for each storm. Since the 25 storms were typically of one to three days duration, only automatic rain data were treated in this way. Cumulative plots were useful for distinguishing errors of timing in some gauge records, as the temporal signature of each storm was reproduced at many gauges.

### Normal rain

Automatic gauges in the Southern Alps are subject to many problems, including freezing in winter, detail lost because of snow at any time of the year, and equipment failure in the harsh conditions; long uninterrupted records are thus rare. Our data on extreme rainfall are a very small geographic sample, as only gauges in a narrow zone just downwind and parallel to the Alpine Fault can measure extremes, and nearly all the gauges in this zone were near Hokitika. All except one of the maxima listed in Table 2 are from these gauges. Daily gauges and storage gauges both within and around the mountains have fewer gaps, but do not measure such high intensities, because of both their location and the time resolution of the data recording. The best we can do at other locations is to examine the data when we arrange them as trans-alpine profiles, perpendicular to the Alpine Fault.

Thirty-year normal rainfalls (1951-80) were derived for each gauge by correlation with the long-term daily records from the nearest locations: Hokitika, Franz Josef, Haast or Milford, which are all NW of the Main Divide. Where available, published normals have been used (New Zealand Meteorological Service, 1983). When correlating storage data with daily data, the time partition of the storage gauge readings was used; these partition times are invariably during fine weather, so each correlation pair represents one or more complete storms. When correlating the other data, a



**TABLE 2** – The maximum Southern Alps intensities for each duration plotted on Figure 4, except for Alex Knob. All except one of these maxima are from gauges on the Hokitika trans-alpine profile, because there are very few long-term gauges in the zone of highest rainfall elsewhere in the Southern Alps. Start Date is at the beginning of the period of stated duration.

Site	Duration	Depth (mm)	$P_{\max}$ (mm/hr)	$X_{0.5}$ ( $\text{mm}^{1.5}/\text{hr}$ )	Start Date (yyymmdd)
Waterfall at Cropp	6 min	16.7	167	53	881206
Waterfall at Cropp	10 min	20.1	121	49	880519
Waterfall at Cropp	20 min	33.3	100	58	880519
Waterfall at Cropp	30 min	44.5	89.0	63	880519
Waterfall at Cropp	1 hour	77.0	77.0	77	880519
Waterfall at Cropp	2 hours	129.5	64.8	92	880519
Prices Flat at Hokitika	6 hours	325.4	54.2	133	780512
Prices Flat at Hokitika	12 hours	566.3	47.2	163	780511
Waterfall at Cropp	1 day	758.0	31.6	155	891227
Waterfall at Cropp	2 days	913.0	19.0	132	891226
Waterfall at Cropp	3 days	1057	14.7	125	891213
Luncheon Rock at Waiho	4 days	1136	11.8	116	830109
Rapid Ck at Hokitika	5 days	1272	10.6	116	690903
Rapid Ck at Hokitika	7 days	1433	8.5	111	690903
Waterfall at Cropp	14 days	1911	5.7	104	891214
Waterfall at Cropp	1 month	2845	3.9	105	841121
Waterfall at Cropp	2 months	4684	3.2	123	841113
Waterfall at Cropp	3 months	5939	2.7	127	841013
Tuke Hut at Tuke	4 months	6879	2.4	127	880721
Waterfall at Cropp	6 months	9148	2.1	138	840714
Waterfall at Cropp	1 year	14403	1.6	154	821105

monthly partition was used, and some storms straddle the partition times. Correlations were reasonable along each trans-alpine profile within 50 km of the correlating gauge ( $0.95 > R^2 > 0.55$ ), i.e. to southeast of the Main Divide. The value of normal rain at each gauge was calculated as the ratio of rainfall at the gauge to rainfall at the reference site over the period when both gauges operated, multiplied by the normal rain at the reference site.

## Results

### Rain extremes

Figure 4 shows the largest  $X_{0.5}$  ( $=P_{\max}/D^{0.5}$ ) values from the Southern Alps for a range of durations from six minutes to one year. The world maxima

data reported by Paulhus (1965) and updated in World Meteorological Organisation (1994) are plotted for comparison. For each Southern Alps category (short duration, checked, and long duration) data values from other storms between the cut-off  $X_{0.5} \geq 50$  or 100 and the maximum value are shown. A number of the short duration maxima are not supported by other data and must be suspect.

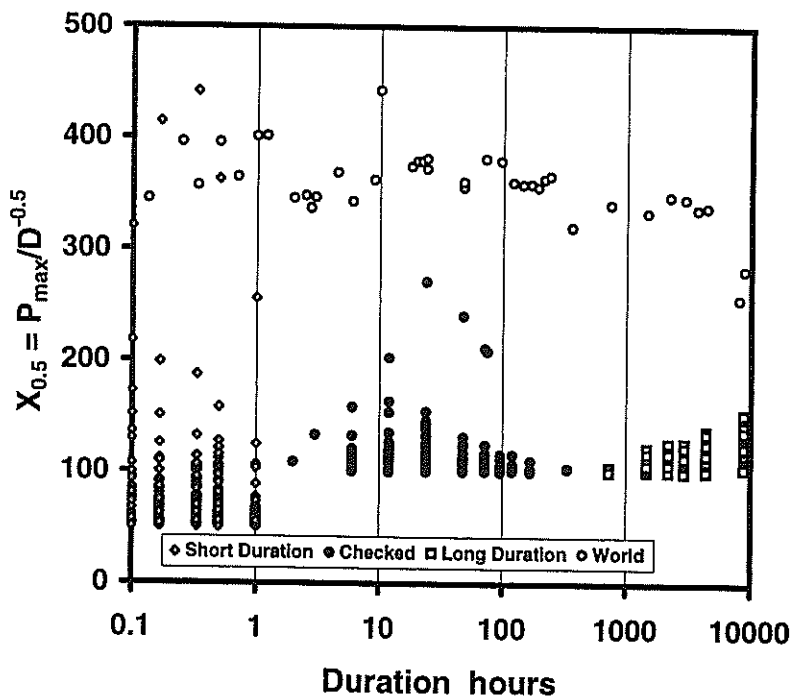


**FIGURE 4** – Maximum rain intensity divided by the square root of duration versus duration in the Southern Alps, NZ. Other data are maxima for the world (Paulhus, 1965; World Meteorological Organisation, 1994), and for Alex Knob for a storm in March 1982. Data for durations of 2 hours to 14 days have been checked against other sites (see text).

The maximum  $X_{0.5}$  values between 3 hours and 72 hours are from a 3-m storage gauge operated by the Westland National Park Board, at an elevation of 1200 m on the south side of the Waiho valley near Franz Josef, in March 1982. The three-day storm total of 1810 mm is a record for New Zealand. Another storage gauge at Luncheon Rock (79 km NW) overflowed after 1310 mm of rain, and provides supporting evidence for this large

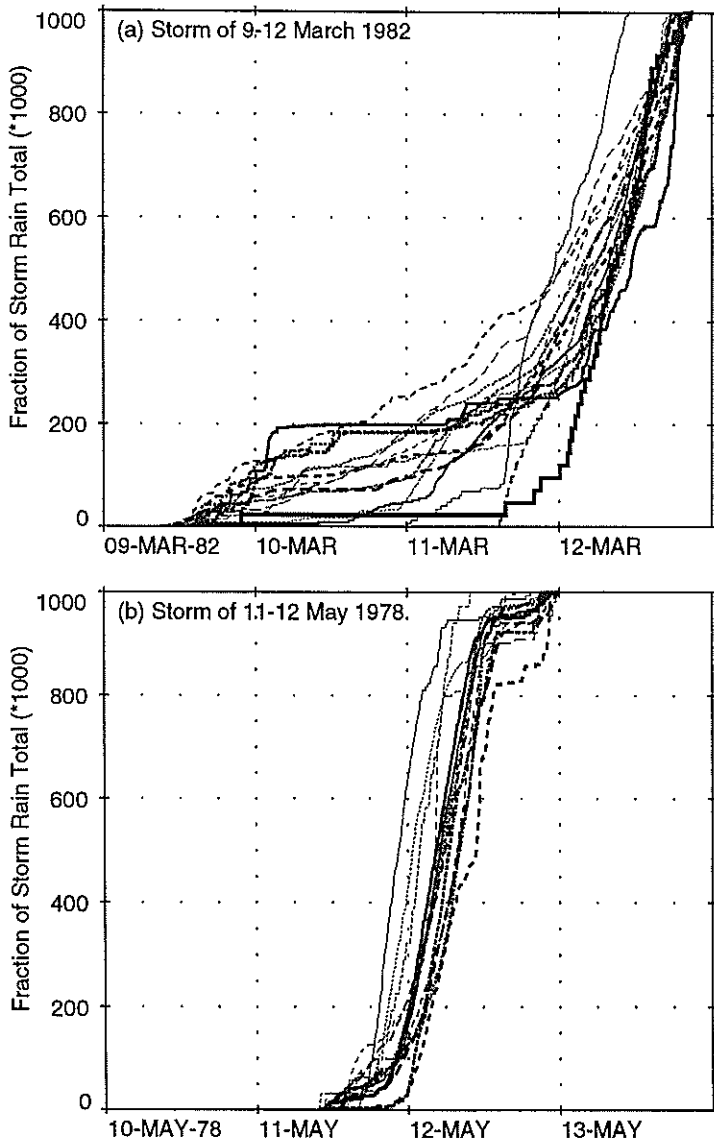


**FIGURE 5** – Cumulative rainfall (per thousandth part of total storm rainfall at each gauge) of the four storms with the largest values of  $X_{0.5}$ . Gauges are plotted with increasing line thickness for increasing northeast distance. The storms have different durations: (a) March 1982-3.25 days; (b) May 1978-1.5 days;

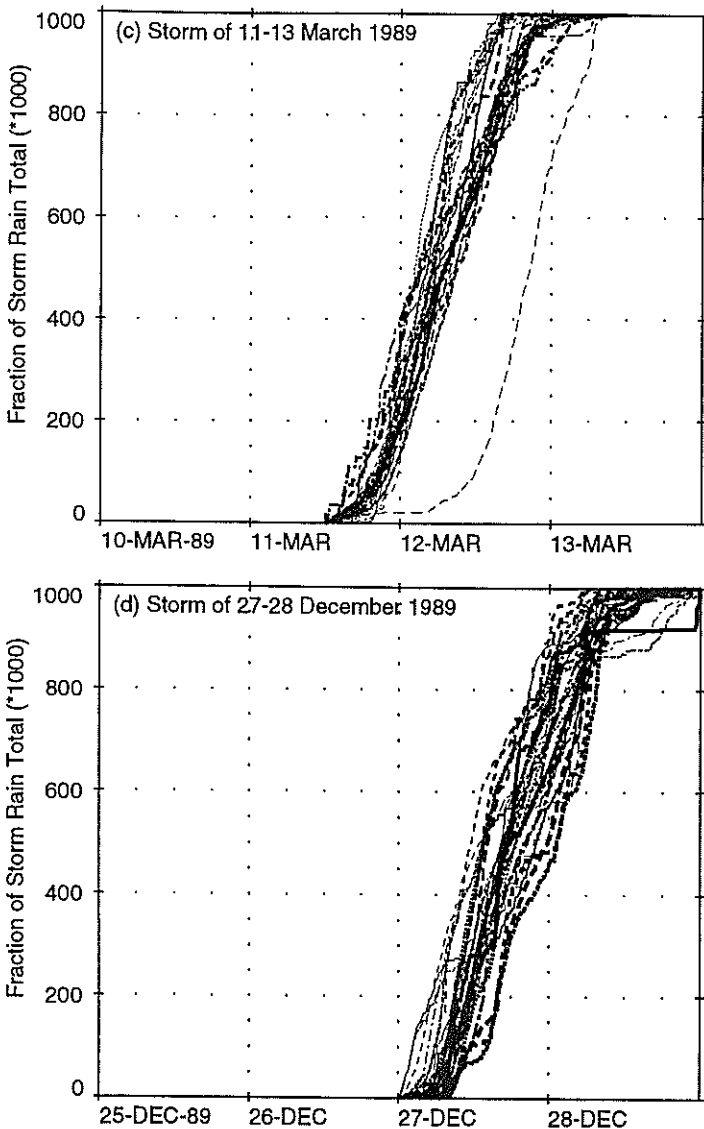


**FIGURE 5** – Cumulative rainfall (per thousandth part of total storm rainfall at each gauge) of the four storms with the largest values of  $X_{0.5}$ . Gauges are plotted with increasing line thickness for increasing northeast distance. The storms have different durations: (c) March 1989-1.5 days; and (d) December 1989-2 days. The March 1989 plot (c) shows a 12-hour timing error at Cassinia Moraine.

quantity. The circumstances surrounding these exceptional rainfalls are described in Henderson (1998). This three-day rainfall at Alex Knob was distributed according to median temporal profiles for the March 1982 storm (Fig. 5a), to give values from 3 hours to 75 hours as listed in Table 3, and plotted on Figure 4.

**TABLE 3** – Tabulation of the Alex Knob data plotted on Figure 4. Depth and intensity values were derived from the median temporal profiles of other gauges from the March 1982 storm.

Duration (hrs)	Depth (mm)	$P_{max}$ (mm/hr)	$X_{0.5}$ ( $mm^{1.5}/hr$ )
3	231	77.0	133
6	388	64.7	159
12	702	58.5	203
24	1331	55.5	272
48	1672	34.8	241
72	1796	24.9	212
75	1810	24.1	209

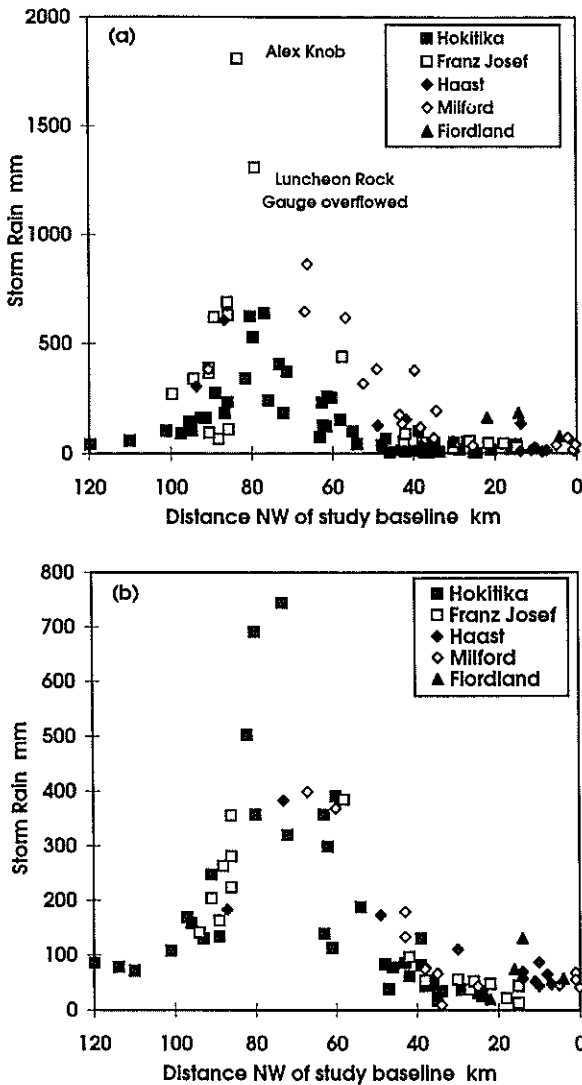
### Temporal patterns of storms

Figure 5 shows the temporal patterns from the recording gauges of the four storms with largest  $X_{0.5}$  values. The gauges have been sorted in ascending order of their distance NE along the Alps from the study area origin (see Fig. 1), and lines of increasing thickness are used on the plot to indicate this order. In Figure 5c one gauge stands out as having a timing error of some 12 hours. Three storms show an accumulation profile in the standard ‘S’ shape, and the storm of 9-12 May 1982 (Fig. 5a) shows an increasing intensity with the maximum towards the end of the storm.

### Trans-alpine profiles - storms

Data from the two storms from Figure 5 with the highest values of  $X_{0.5}$  are presented as rain depths in Figure 6, classified according to the four trans-alpine profile regions shown in Figure 1. Some data from Fiordland are also plotted, as the storm extended further south.

The trans-alpine profile of the May 1978 storm (Fig. 6b) shows the highest rainfalls between 55 and 85 km NW of the study baseline. Only the Hokitika trans-alpine profile had enough gauges in this band at that time to identify the location of maximum rainfall, which is between 70 and 80 km NW. The Main Divide and highest ground is at 60 km NW, and the Alpine Fault is at 85 km NW.



**FIGURE 6** – Total storm rainfalls (mm) from the storms of March 1982, (a) and May 1978, (b), from recording and daily gauges. The abscissa is distance NW of the grid origin (see Fig. 1). Gauges are grouped according to their proximity to the trans-alpine profiles shown in Fig. 1, as follows: Hokitika from 550 to 450 km NE; Franz Josef from 450 to 350 km NE; Haast from 350 to 250 km NE; Milford from 250-150 km NE; and the Fiordland group from 150 to 0 km NE accounts for the rest.

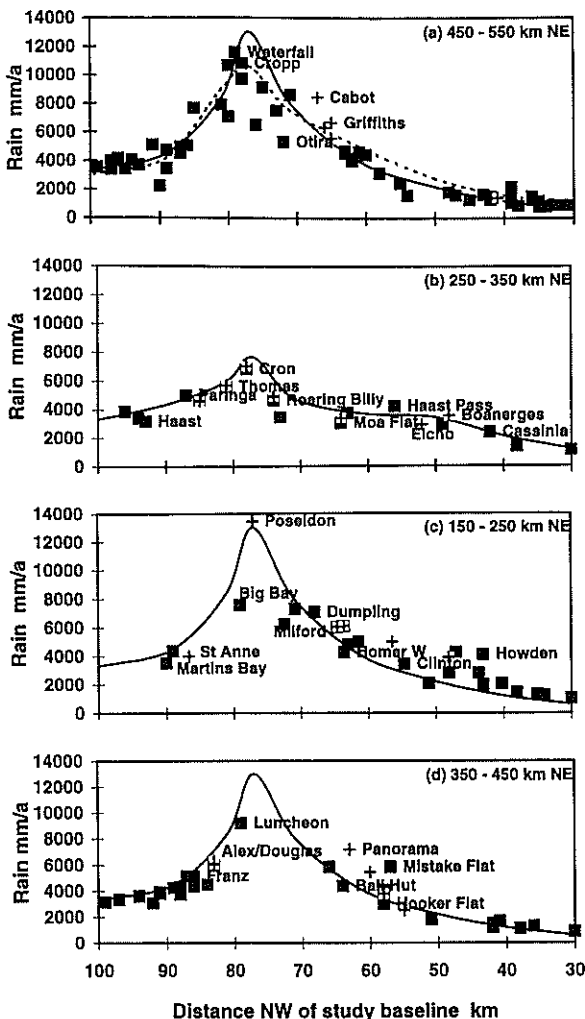


**FIGURE 7** – Rainfall normals 1951-80 (mm/year) of gauges near the Hokitika (a), Haast (b), Milford (c) and Franz Josef (d) trans-alpine profiles. Values have been derived by correlation with a long-term daily gauge at the western end of each trans-alpine profile. Abscissae are as for Figure 6. Gauges plotted as cross (+) are the new gauges, which were installed during the analysis reported here. The solid lines are our best subjective estimate of the “invariant” orographic profile. The same line is used in (a), (c) and (d). The dashed line in (a) is that from Chinn (1979), using data from McSaveney *et al.* (1978).

Trans-alpine profiles of the other 23 storms identified are similar to the two illustrated. The maximum rainfall is located 10-20 km upwind of the highest ground.

### Trans-alpine profiles – normal rain

Figure 7 shows the trans-alpine profiles of normal rain, using daily and storage gauge results as well as data from automatic rain gauges. A line drawn through the middle of the data is our best subjective estimate of the “invariant” orographic profile. The scatter in the data reflects factors such as differences in the direction of the wind, and convective cells embedded in the zone of orographic uplift.

## Discussion

### Rain extremes

For world rain maxima as shown in Figure 4, the intensity measure is relatively invariant,  $X_{0.5} \sim 370$ , over the full range of durations. Values for long-duration maxima are slightly lower, so the best fit line to the current world depth duration data has a value for  $n > 0.5$ .

In the Southern Alps rain maxima are particularly intense for duration 1 day, where  $X_{0.5} = 272$ , and less for both larger (and smaller) durations, with  $X_{0.5} \sim 100$  for duration 14 days. For longer durations  $X_{0.5}$  increases to 154 at 365 days, reflecting a high frequency of storms throughout the year.

The relatively high values of  $X_{0.5}$  for durations near to 1 day represent persistent rain at relatively low intensity, which is a characteristic of

**TABLE 4** – Ratios of Southern Alps (excluding Alex Knob) and Alex Knob rain maxima to World maxima.

For durations around	Southern Alps	Alex Knob
6 min	15%	
1 hour	19%	19%
2 hour	26%	32%
6 hour	39%	46%
12 hour	42%	60%
24 hour	40%	71%
2 days	36%	67%
3 days	33%	55%
1 week	31%	
2 weeks	31%	
1 month	30%	
1 year	54%	



orographic rain generation. The relatively low values for durations near 14 days reflect the common interval between rain events delivered by the global circulation. The relatively high value at 1 year represents frequent rain, which is a characteristic of the maritime climate. However all values are less than world values, presumably because the air at 45 degrees latitude is never as warm as tropical air can be, and so cannot hold as much moisture.

### Temporal patterns of storms

The use of normalised values of accumulated rain for each gauge and each storm allows comparison of the timing of rain and its relative intensity. The dominant influence of the large rain gradients perpendicular to the mountains is removed. Two types of timing signal are evident in Figure 5.

Firstly, there are differences in timing perpendicular to the Alpine Fault. These are illustrated in Figure 5(a). Three gauges; Jollie (plotted as a thin continuous line), Fang Hill (medium dashed line), and Ranger Stream (thick continuous line) have the onset of most intense rain delayed until after mid-day on the 11<sup>th</sup> March. These three gauges are the most south-easterly of those plotted in Figure 5(a), and indicate that in some storms, rain does not get far downwind of the Main Divide until a front has passed.

Secondly, differences in timing of rainfall along the length of the Southern Alps can be observed. The two earlier storms, those of May 1978 (Fig. 5b) and March 1982 (Fig. 5a), exhibit a systematic progression of the onset of intense rain, which begins at the SW end, and progresses NE along the Alps. This progression is most obvious in Fig 5(b), where the thin lines are for gauges near Milford, and show the rain starting six hours earlier than the gauges along the Hokitika trans-alpine profile. The two 1989 storms (Figs 5c and 5d) show a high degree of consistency in both temporal pattern and timing of rainfall. Of the 21 other storms analysed, thirteen had a near simultaneous pattern, and eight showed a progressive onset from SW to NE. The peak flows in hydrographs of river flow from the Southern Alps sometimes show this progression, including the largest peaks ever measured (McKerchar *et al.*, 1997, Fig. 4.1). This progression is caused by the passage of a front of cold air from the south, causing an uplift of warmer air from the northwest that is additional to the orographic uplift. Rain stops after the passage of the cold front.

Fronts generally take less than 12 hours to progress 400 km. The onset of the most intense rain over NE distances less than 100 km (i.e. the width of the largest basins draining the Main Divide) is therefore less than 3 hours, and may be considered 'simultaneous'.

### **Trans-alpine profiles - storms**

When storm profiles (Fig. 6) are compared to the normal profiles (Fig. 7) they seem very similar. The normal profile is just the sum of many similar storm profiles.

Some storms produce relatively more rain northwest of the Main Divide than normal, and other storms spill more of their rain over the divide. Indeed the proportion has been observed to change during a storm (Sinclair *et al.*, 1997). These differences are important, because only rain falling south-east of the divide can be used for hydroelectric generation and irrigation. These differences are obvious when the storm rain is scaled with the normal rain at each location, but when storm rain alone is plotted they are obscured by the steep spatial gradient.

### **Trans-alpine profiles – normal rain**

Along the Hokitika trans-alpine profile, the data in Figure 7a confirm the profile derived from the data of McSaveney *et al.* (1978) and shown in Chinn (1979), which is plotted. New data are available from gauges in the Wilberforce headwaters (Griffiths and Cabot gauges on Fig. 7a) at low and high altitude respectively; these short records support the general profile shape for a region where there were no previous data.

Along the Haast trans-alpine profile (Fig. 7b) the results from short-term recording gauges agree very well with those of long-term storage data (crosses on top of filled squares), indicating that records of a few years can give a reliable picture of the mean rain distribution. The Haast gauges show a lesser maximum at a similar distance from the Alpine Fault to the Hokitika maximum. This indicates that the location of the maximum is invariant with respect to the Alpine Fault, but suggests that its magnitude is related to the barrier height downwind. The barrier is substantially lower at Haast (see Fig. 2).

Initially the Milford trans-alpine profile (Fig. 7c) did not have any gauges seaward of Milford (67 km NW), where the highest reliable values for rainfall on this profile had been recorded. Analogy with the Hokitika profile suggested that the maximum would be 10 km seaward of Milford, and would be of the same order as the Hokitika maximum, since the highest ground along the Milford profile is of similar altitude (see Fig. 2). A new gauge (Poseidon) was installed at this location, and 12 months data confirmed this suggestion, with an estimated normal annual rainfall of over 12 m ( $R^2$  with weekly Milford rain = 0.93) at the Poseidon gauge site.

At Franz Josef (Fig. 7d), the results for peak trans-alpine profile rain are not conclusive. We have automatic gauges at Alex Knob and Douglas Hut, which are the same NW distance (2 km) from the Alpine Fault, but differ in altitude by 1200 m, and both have a normal of 6 m/year. A third automatic

gauge at Luncheon Rock is 4 km further away from the Alpine Fault, and its normal is 9 m/year, showing that distance from the Alpine Fault is still the predominant variable determining rain in this region. The higher elevation of the Main Divide along this trans-alpine profile suggests that the maximum rain here will be greater than at any other place in the Southern Alps.

## Conclusions

The rain maxima occurred during storms that produced widespread rain throughout the 400-km long area and beyond. The onset and end of this rain was almost simultaneous throughout this large area. We conclude that these rain maxima occurred when a mass of moist air, at least 400 km across, moved onto the mountain barrier.

The depth-duration curve of Southern Alps rain maxima differs from that for world maxima, with peaks around durations of one day and one year, and a trough around a duration of two weeks. We conclude that 1 day is the typical time for a mass of moist air to cross the mountain barrier, and that 2 weeks is the typical period between recurring synoptic weather patterns. The 1-year maximum is because periods of airflow from the northwest are frequent; and we did not analyse longer durations, which may have even larger values.

The onset and cessation of intense rainfall may be largely simultaneous over the largest basins draining the Main Divide. We conclude that we can use this to detect errors of timing and missing data.

Storm rain depth profiles across the mountain barrier have a similar shape to the normal rain profile. We conclude that there is a narrow zone ~ 10 km wide where all the maxima are observed; it is centered approximately 10 km southeast of the Alpine Fault and well upwind of the highest ground.

The maximum rain intensity in this narrow zone seems to be related to the height of the Main Divide in the vicinity. We have only 400 station-years of data from gauges in this maximum rain zone and so the sample of extreme intensities is small. Temporal correlation of rain depths between gauges along the trans-alpine profiles is very high. We conclude that identification of the most intense rain events is reliable, but direct observation of the most intense rain within those events is very rare.

## Acknowledgements

Financial support for the analysis reported here was provided by the Public Good Science Fund (Contracts CO1418 and CO1514), administered by New Zealand's Foundation for Research Science and Technology. NIWA field teams at Dunedin, Alexandra, Tekapo, Christchurch and Greymouth and some Regional Council staff have collected data. Regional Councils

and the Waitaki Hydro Group of the Electricity Corporation of New Zealand also provided data. NIWA Greymouth and Dunedin field teams installed the new gauges at Franz Josef, Haast and Milford. The Fiordland National Park staff at Te Anau provided the daily data for the 1980s from their huts on the Milford Track and elsewhere, and the re-processing of these data by Sally Nielsen has provided increased confidence in its quality. Charles Pearson and Alistair McKerchar provided valuable guidance through internal reviews. Constructive comments by the referees have also contributed to the final result.

## References

- Adams, J.E. 1980: Contemporary Uplift and Erosion of the Southern Alps, New Zealand. *Geological Society of America Bulletin Part II*, v.91: 1-114.
- Anderton, P.W. 1973: The Significance of Perennial Snow and Ice to the Water Resources of the South Island, New Zealand. *Journal of Hydrology (NZ)* 12(1): 6-18.
- Chinn, T.J. 1979: How wet is the wettest of the wet West Coast? *New Zealand Alpine Journal* 32: 85-88.
- Coulter, J.D. 1973: A Water Balance assessment of the New Zealand Rainfall. *Journal of Hydrology (NZ)* 12(2): 83-91.
- Duncan, M.J. 1992: How much does it rain in the Hokitika catchment? *New Zealand Hydrological Society Symposium (Auckland, NZ)*, New Zealand Hydrological Society.
- Electricity Shortage Review Committee 1992: *The Electricity Shortage 1992*. The Department of Prime Minister and Cabinet, Wellington, New Zealand.
- Grant, P.J. 1969: Rainfall Patterns on the Kaweka Range. *Journal of Hydrology (NZ)* 8(1): 17-34.
- Griffiths, G.A.; McSaveney, M.J. 1983: Distribution of mean annual precipitation across some steep-land regions of New Zealand. *New Zealand Journal of Science* 26: 197-209.
- Henderson, R.D. 1993: Extreme Storm Rainfalls in the Southern Alps, New Zealand. In: Kundzewicz *et al.* (eds.) *Extreme Hydrological Events: Precipitation, Floods and Droughts* (Proceedings of the Yokohama Symposium, July 1993). *IAHS Publication No. 213*: 113-120.
- Henderson, R.D. 1998: The Southern Alps Experiment or Why is the West Coast as wet as the West Coast is? *New Zealand Alpine Journal*, 1998: 106-109.
- Hessell, J.W.D. 1982: The Climate and Weather of Westland. *New Zealand Meteorological Service Miscellaneous Publication 115(10)*. Ministry of Transport, Wellington, New Zealand.

- Jowett, I.G.; Thompson, S.M. 1977: Clutha Power Development Flows and Design Floods, 114 p, In: Environmental Impact Report on Design and Construction Proposals, Government Printer, Wellington, New Zealand, 1978
- McKerchar, A.I.; Ibbitt, R.P.; Woods, R.A. 1997: Analysis and estimation of extreme events: deterministic methods. In: Mosley, Paul; Pearson, Charles (eds.). *Floods and Droughts: the New Zealand experience*. New Zealand Hydrological Society, Wellington, New Zealand, p. 51-63.
- McSaveney, M.J. 1978: The Pastoral Scene: The Magnitude of Erosion across the Southern Alps, *Proceedings of the Conference on Erosion Assessment and Control in New Zealand*, 21-25 August 1978, New Zealand Association of Soil Conservators.
- McSaveney, M.J.; Chinn, T.J.; Horrell, G.A.; Longson, C.K. 1978: The Measured Distribution of Precipitation across the Southern Alps, *New Zealand Hydrological Society Symposium*, Wellington, New Zealand.
- National Water and Soil Conservation Organisation 1970-75: Ivory Glacier, Representative Basin for Glacial Region. *Hydrological Research Annual Reports Nos. 5, 28, 35 & 36*, National Water and Soil Conservation Organisation, Wellington, New Zealand.
- New Zealand Meteorological Service 1983: Rainfall Normals for New Zealand 1951 to 1980. *New Zealand Meteorological Service Miscellaneous Publication 185*, Ministry of Transport, Wellington, New Zealand.
- Paulhus, J.L.H. 1965: Indian Ocean and Taiwan Rainfalls Set New Records. *Monthly Weather Review* 93(5): 331-335.
- Raudkivi, A.J. 1979: *Hydrology*, Pergamon, Oxford. p 82.
- Rodda, J.C. 1995: Capturing the hydrological cycle 1995: In: Kite (ed.) *Time and the River*. Water Resources Publications, Fort Collins, USA, p. 25-28.
- Rodgers, M.W.; Thompson, S.M. 1992: *Tideda Reference Manual 2nd ed.* Publication No 24, Hydrology Centre, National Institute of Water and Atmospheric Research, Christchurch, New Zealand.
- Shaw, E.M. 1983: *Hydrology in Practice*, Van Nostrand Reinhold (UK), Wokingham, England.
- Sinclair, M.R.; Wratt, D.S.; Henderson, R.D.; Gray, W.R. 1997: Factors affecting the distribution and spillover of precipitation in the Southern Alps of New Zealand - a case study. *Journal of Applied Meteorology* 36: 428-442.
- Stephen, G.D. 1972: *The Water Resources of the Rakaia Catchment*. North Canterbury Catchment Board and Regional Water Board, Christchurch, New Zealand. 41 p and Appendix of Daily Mean Flows.
- Tomlinson, A.I. 1980: *The Frequency of High Intensity Rainfalls in New Zealand*. Water and Soil Technical Publication 19, Ministry of Works and Development, Wellington, New Zealand.

- Walter, K.M. 1990: *Index to Hydrological Recording Sites in New Zealand 1989*. Publication No. 21, Hydrology Centre, Christchurch, New Zealand.
- Wellman, H.W. 1979: An uplift map for the South Island of New Zealand and a model for the uplift of the Southern Alps. In Walcott, R.I. and Cresswell, M.M. (eds.), *The Origin of the Southern Alps*, Royal Society of New Zealand Bulletin 18: 13-20.
- Whitehouse, I.E. 1985: The frequency of high-intensity rainfalls in the central Southern Alps, New Zealand. *Journal of the Royal Society of New Zealand* 15(2): 213-226.
- World Meteorological Organisation, 1994: *Guide to Hydrological Practices: data acquisition and processing, analysis, forecasting and other applications*. 5<sup>th</sup> edition. World Meteorological Organisation, Geneva.